

β - γ VIBRATIONS AND SU_3 SYMMETRY IN THE FERMION
DYNAMICAL SYMMETRY MODEL

CHENG-LI WU*

*Department of Physics and Astronomy, University of Tennessee, Knoxville, Tennessee 37996-1200;
Department of Physics and Atmospheric Science, Drexel University, Philadelphia,
Pennsylvania 19104-9984, USA*

MIKE W. GUIDRY

*Department of Physics and Astronomy, University of Tennessee, Knoxville, Tennessee 37996-1200,
USA*

DA HSUAN FENG and JIN QUAN CHEN*

*Department of Physics and Atmospheric Science, Drexel University, Philadelphia,
Pennsylvania 19104-9984, USA*

Received 10 October 1989

UDC 539.142

Original scientific paper

In addition to the previously established equivalence between the Fermion Dynamical Symmetry Model (FDSM) and the particle-rotor model, it is found that different β - γ vibrational states in the geometrical description correspond to different SU_3 representations in the FDSM, and that there is a one-to-one correspondence between β - γ vibration quantum numbers (n_β, n_γ, K) and the SU_3 quantum numbers (λ, μ, κ). It is shown that the excitation energy associated with the SU_3 Casimir operator can be written as $\hbar\omega (n_\gamma + n_\beta + K/2) \times (1 + 0(1/n_1))$, where n_1 is the number of particles in the normal-parity valence levels. In the large n_1 limit, this becomes identical to the geometrical results, provided the β - γ vibrational frequency now is given as $\hbar\omega = 3B_2n_1$, where B_2 is the strength of the n-p qua-

* Permanent address: Department of Physics, Jilin University, People's Republic of China.

* Permanent address: Department of Physics, Nanjing University, People's Republic of China.

drupole-quadrupole interactions. Experimental data for the first β - and γ -band band-head energies in the actinide region seem to support this identification. The sudden drop of the first γ -band band-head for $N > 151$ nuclei provides additional evidence for the dynamical Pauli effect predicted by the FDSM.

1. Introduction

Recently a microscopic nuclear model for low lying collective motion, the Fermion Dynamical Symmetry model (FDSM), was proposed¹⁾. This model is basically a spherical shell model in a symmetry-dictated truncated space, in which shell model calculations for heavy nuclei become tractable, and which has dynamical symmetry limits where analytical solutions can be obtained. Depending on which valence shell the nucleons occupy, nuclei may have either Sp_6 or SO_8 symmetries, and have the dynamical symmetry chains shown in Fig. 1.

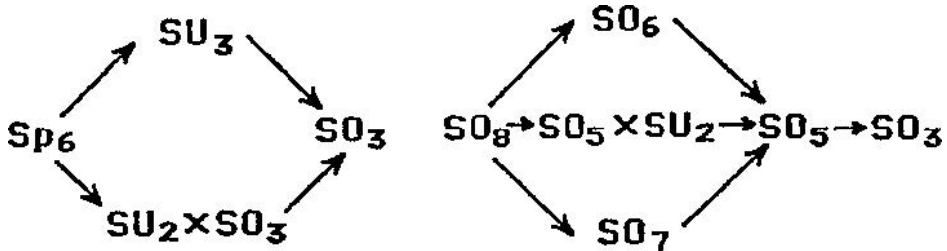


Fig. 1. The group chains of the Sp_6 and SO_8 symmetries.

Each symmetry limit of the FDSM solutions corresponds to a known collective mode of nuclear motion²⁾: $Sp_6 \supset SU_3$, the rotational mode; $SO_8 \supset SO_6$, the γ -soft mode; $Sp_6 \supset SU_2$ and $SO_8 \supset SO_5 \times SU_2$, the vibrational modes for Sp_6 and SO_8 nuclei, respectively. There is a new vibrational mode, the $SO_8 \supset SO_7$ mode, predicted first by Ginocchio³⁾ and confirmed by the FDSM, which differs from the other vibrational modes by a linear particle number dependence of the energy spacing in spectra, and by different Pauli factors in $B(E2)$'s and other physical quantities. Experimental evidence for this new vibrational mode was soon recognized in the Ru and Pd region⁴⁾.

It has been shown that all the boson dynamical symmetries of the Interacting Boson Model (IBM)⁵⁾ can be obtained from the FDSM if the Pauli effects are neglected by assuming the shell degeneracy of normal-parity levels $\Omega_1 \rightarrow \infty$, with $\Omega_1 = \sum (2j + 1)/2$, where the sum is over normal-parity orbitals⁶⁾. In fact, one can even use the FDSM computer code⁷⁾ to obtain IBM2 results if the realistic shell degeneracy Ω_1 is artificially replaced by a sufficiently large number for both protons and neutrons. The relationship between the FDSM and the IBM is showed in Table 1. Thus the IBM is the large shell limit of the FDSM. Of course the realistic shell degeneracy is not very large and Pauli effects must come to play a role when many particles fill the shells. Experimental evidence of such Pauli effects has been found and agrees with the predictions of the FDSM⁸⁾. For example, the saturation of the $B(E2; 2 \rightarrow 0)$'s in rare-earth nuclei when the neutron num-

ber approaches $N = 99$, where the corresponding valence neutron number in normal-parity levels is $2\Omega_1/3$, is due to such an effect; we call this the dynamical Pauli effect⁹⁾.

TABLE 1.

FDS	Collective mode	IBM
$Sp(6) \supset SU(3)$	$\rightarrow \leftarrow$ Rotation	$\rightarrow \leftarrow U(6) \supset SU(3)$
$SO(8) \supset SO(6)$	$\rightarrow \leftarrow$ γ -Soft	$\rightarrow \leftarrow U(6) \supset SO(6)$
$Sp(6) \supset SU(2) \times SO(3)$ $SO(8) \supset SO(5) \times SU(2)$ $SO(8) \supset SO(7)$	$\rightarrow \leftarrow$ Vibration	$\rightarrow \leftarrow U(6) \supset U(5)$

The comparison of dynamical symmetry limits for the FDSM and the IBM, and their corresponding modes of nuclear collective motion.

Because of the difficulties of applying the spherical shell model to a heavy system, the collective motion of heavy nuclei has been traditionally described by the phenomenological Geometrical Model (GM), developed by the Copenhagen school¹⁰⁾, and associated microscopic approaches based on the deformed mean field approximation such as the cranked shell model or cranked HFB¹¹⁾. This approach has been very successful in understanding heavy nuclear structure, and is still the best quantitative description one can apply to a heavy system. Nevertheless, it would be highly desirable to describe the nuclear collective motion via the spherical shell model without introducing the classical concept of deformation, or to go beyond the deformed mean field approximation to restore symmetries and many-body correlations. There are new developments in the second direction implemented by improving the HFB technique; this is the VAMPIRE Program¹²⁾. The FDSM is a prescription for spherical shell model solutions in heavy nuclei which may be regarded as a development in the first direction.

In previous publications we have shown how the FDSM can describe the phenomena normally explained by the geometrical model in terms of deformations, but using the spherical shell model language. This demonstration is important, on one hand, to check whether the FDSM has the same capability as the GM to explain nuclear collective phenomena; on the other hand, it provides a deeper understanding of the microscopic quantities which control these phenomena, including nuclear deformation itself, since neither classical quantities, such as deformation, nor symmetry breaking, such as rotational symmetry breaking or number conservation breaking, are introduced in the FDSM. In this paper, we shall add another aspect to this study by discussing the correspondence of the β - γ vibrations in the FDSM and GM.

In the following section we shall first present the FDSM Hamiltonian for an n-p system, followed by a comparison between the particle-rotor model and the FDSM SU_3 Hamiltonian. A general proof of the equivalence of these two model, and the correspondence between the β - γ vibrational states in the GM and the different SU_3 representations in the FDSM, is given in section 3. In section 4 a comparison with experimental data will be presented, and the dynamical Pauli

effect (which causes a sudden drop of the first γ -band band-head in the actinide region) will be discussed. Finally, section 5 is a brief summary.

2. The FDSM Hamiltonian

In the FDSM the separation of collective degrees of freedom is achieved through a special k - i decomposition of the single-particle angular momentum, $\mathbf{j} = \mathbf{k} + \mathbf{i}$. The integer part \mathbf{k} is called the pseudo-orbital angular momentum, and the half-integer part \mathbf{i} is called the pseudo-spin. The decomposition is such that one part must be either $\mathbf{k} = 1$ or $\mathbf{i} = 3/2$, which is called the active part and is responsible for two identical particles to form coherent S and D pairs (the pairs with angular momentum 0 and 2), and thus can be viewed as the collective degrees of freedom; the other part is called the inert part, which tends to couple to zero in the low energy regime. This is a natural generalization of the pairing model. The pairing model assumes that for an identical nucleon pair the nuclear force tends to couple the single-particle angular momenta \mathbf{j} to zero. In the FDSM it is assumed that, not the total \mathbf{j} , but only its inert part tends to couple to zero, leaving a small active part (either $\mathbf{k} = 1$ or $\mathbf{i} = 3/2$), which allows two identical nucleons to form a collective S pair or a D pair. Therefore, instead of the ground state being described as an S pair condensate as in the pairing model, in the FDSM the entire set of low-lying collective bands is described by an S - D pair condensate.

It can be shown that this decomposition is unique within one major shell. A reclassification of the shell model basis in terms of k and i quantum numbers is shown in Table 2 (for details see Ref. 2). With this k - i decomposition a k - i basis $\mathbf{b}_{km_k i m_i}^{\sigma \dagger}$ ($\sigma = \pi, \nu$ denotes proton or neutron, respectively) can be defined as a linear superposition of the original shell model single-particle orbitals $a_{jm}^{\sigma \dagger}$

$$\mathbf{b}_{km_k i m_i}^{\sigma \dagger} = \sum_j \langle k m_k i m_i | j m \rangle a_{jm}^{\sigma \dagger} \quad (2.1)$$

The coherent S and D pairs and the multipole operators are defined as

$$\mathbf{S}^{\sigma \dagger} = \sqrt{\Omega_{ki}^{\sigma}}/2 [\mathbf{b}_{ki}^{\sigma \dagger} \mathbf{b}_{ki}^{\sigma \dagger}]_{00}^{00}, \quad \mathbf{D}_{\mu}^{\sigma \dagger} = \sqrt{\Omega_{k3/2}^{\sigma}}/2 [\mathbf{b}_{k3/2}^{\sigma \dagger} \mathbf{b}_{k3/2}^{\sigma \dagger}]_{0\mu}^{02}, \quad \mathbf{D}_{\mu}^{\sigma \dagger} = \sqrt{\Omega_{i1}^{\sigma}}/2 [\mathbf{b}_{i1}^{\sigma \dagger} \mathbf{b}_{i1}^{\sigma \dagger}]_{\mu 0}^{20},$$

(for any k and i) (for i -active) (for k -active) (2.2)

$$\mathbf{P}_{r\mu}^{\sigma}(k) = \sqrt{\Omega_{ki}^{\sigma}}/2 [\mathbf{b}_{ki}^{\sigma \dagger} \tilde{\mathbf{b}}_{ki}^{\sigma \dagger}]_{\mu 0}^{r0}, \quad \mathbf{P}_{r\mu}^{\sigma}(i) = \sqrt{\Omega_{ki}^{\sigma}}/2 [\mathbf{b}_{ki}^{\sigma \dagger} \tilde{\mathbf{b}}_{ki}^{\sigma \dagger}]_{0\mu}^{0r} \quad (2.3)$$

where $\Omega_{ki} = (2k + 1)(2i + 1)/2$. If there is more than one i in the normal-parity levels for the k -active case (e. g. shell 7 and shell 8; see Table 2), the right hand side of the equation for $\mathbf{P}_{r\mu}^{\sigma}(k)$ and Eq. (2.2) have an implied sum over i 's. In principle, if there is more than one k in the normal-parity levels for the i -active case the right hand side of $\mathbf{P}_{r\mu}^{\sigma}(i)$ and Eq. (2.2) should also be summed over k 's; practically, there is always only one k value for each shell unless one goes to shells heavier than shell 8 (see Table 2).

TABLE 2.

No.	1	2	3	4	5	6	7	8
n	0	1	2	3	3 4	4 5	5 5 6	6 6 7
k	0	1	1	0	1 0	2 0	1 1 0	1 1 0
i	$\frac{1}{2}$	$\frac{1}{2}$	$\frac{3}{2}$	$\frac{7}{2}$	$\frac{3}{2}$ $\frac{9}{2}$	$\frac{3}{2}$ $\frac{11}{2}$	$\frac{1}{2}$ $\frac{7}{2}$ $\frac{13}{2}$	$\frac{2}{3}$ $\frac{9}{2}$ $\frac{15}{2}$
configuration	$s_{1/2}$	$p_{1/2}$ $p_{3/2}$	$s_{1/2}$ $d_{3/2}$ $d_{5/2}$	$f_{7/2}$	$p_{1/2}$ $g_{9/2}$ $p_{3/2}$ $f_{5/2}$	$s_{1/2}$ $h_{11/2}$ $d_{3/2}$ $d_{5/2}$ $g_{7/2}$	$p_{1/2}$ $f_{5/2}$ $i_{13/2}$ $p_{3/2}$ $f_{7/2}$ $h_{9/2}$	$s_{1/2}$ $g_{7/2}$ $i_{15/2}$ $d_{3/2}$ $g_{9/2}$ $d_{5/2}$ $i_{11/2}$
sym			$G_6 G_8 G_3$		$G_6 G_8 G_3$	G_8	G_6	G_6
Ω_0	0	0	0	0	5	6	7	8
Ω_1	1	3	6	4	6	10	15	21
n'	2	8	20	28	50	82	126	184

Reclassification of Shell Model Single-Particle Basis.

No. labels the shell ordering; n, k, i label the principle, pseudo-orbit and pseudospin quantum numbers; Ω_0 and Ω_1 are the pair degeneracies of the abnormal-parity and normal-parity levels for each shell. The number n' is the maximum allowable nucleon number up to and including that particular major shell. The symbols G_6, G_8 and G_3 are short-hand notation for the symmetries:

$$G_6 = (Sp_6^k \times SO_3^i) \times (SU_2 \times SO_3) \quad (k\text{-active})$$

$$G_6 = (SO_6^i \times SO_3^k) \times (SU_2 \times SO_3) \quad (i\text{-active})$$

$$G_6 = (SU_6^k \times SO_3^i) \times (SU_2 \times SO_3) \quad (k/i\text{-active})$$

where SO_6^k, SO_3^i and SO_3 denote the rotational groups associated with angular momenta k, i and j_0 (abnormal), respectively.

Depending on which shell is the valence shell, a like-particle system could be either k -active ($k = 1$) or i -active ($i = 3/2$). By assuming the inert part of the single-particle angular momentum of each identical particle pair to couple to zero, an S - D fermion pair sub-space is separated out, and the normal-parity levels possess $Sp_6 (SO_6)$ symmetry, with the S - D pair creation and annihilation operators and the associated multipole operators $P_{r\mu}^\sigma(k)$ ($P_{r\mu}^\sigma(i)$) forming a closed algebra. In this truncation the abnormal-parity level has only S pairs and possesses SU_2 -symmetry. Taking this S - D sub-space as a model space the FDSM Hamiltonian is then a linear combination of scalars constructed from the generators of the algebra, and has multiple dynamical symmetry chains as shown in Fig. 1.

For the Sp_6 symmetry the collective degrees of freedom are associated with the pseudo orbital k of the normal parity-levels since the collective motion is carried by those S and D pairs whose pseudo-spin i couples to zero, leaving only k

active. The multipole operators coupled from \mathbf{k} , $\mathbf{P}_{r\mu}^\sigma(k)$ can then be interpreted as collective multipole operators. When i degrees of freedom and $i_0 = j_0$ of the abnormal-parity level are activated (not coupled to zero), we obtain the FDSM equivalent of pair breaking. The number of unpaired particles is called the *heritage number* u in the FDSM; it should be distinguished from the seniority number, which is the number of particles which do not form S pairs. Thus, the pseudo spin \mathbf{i} , and \mathbf{j}_0 of the abnormal-parity level, can be regarded as unpaired single-particle degrees of freedom; the corresponding multipole operators with \mathbf{i} (including $i = j_0$) not coupled to zero, denoted as $\mathbf{P}_{r\mu}^\sigma(b)$, are the multipole operators for unpaired particles,

$$\mathbf{P}_{r\mu}^\sigma(b) = [\mathbf{b}_{ki_1}^{\sigma\dagger} \tilde{\mathbf{b}}_{ki_2}^\sigma]_\mu^{(Kr)I} \tag{2.4}$$

where b is a configuration index, $b \equiv (kk) K(i_1 i_2) I$, with the inert part not coupled to zero, i. e. $I \neq 0$ for k -active. For the abnormal-parity level, $b \equiv (00) 0(j_0 j_0) r$, and we simply denote the abnormal-parity configuration by $b = j_0$. For SO_8 symmetry the situation is reversed: \mathbf{i} is associated with the collective degrees of freedom, while \mathbf{k} and \mathbf{j}_0 are the unpaired single-particle degrees of freedom, since now it is \mathbf{i} which is active in forming coherent S and D pairs. The multipole operators of unpaired particles in this case still have the form of Eq. (2.4), but with $K \neq 0$ except for $b = j_0$.

Upon including the unpaired single-particle degrees of freedom and single-particle energy splitting, the most general FDSM Hamiltonian with two-body effective interactions can be written as follows:

$$\mathbf{H}_{FDS} = \mathbf{H}^\pi + \mathbf{H}^\nu + \mathbf{H}^{\pi\nu} \tag{2.5a}$$

$$\begin{aligned} \mathbf{H}^\sigma = & \sum_j e_j^\sigma \mathbf{n}_j^\sigma + \sum_{\varphi\varphi'} B_0^\sigma(\varphi, \varphi') \mathbf{N}_\varphi^\sigma \mathbf{N}_{\varphi'}^\sigma + \sum_{\varphi\varphi'} G_0^\sigma(\varphi, \varphi') \mathbf{S}^{\sigma\dagger}(\varphi) \mathbf{S}^\sigma(\varphi') + \\ & + G_2^\sigma \mathbf{D}^{\sigma\dagger} \mathbf{D}^\sigma + \sum_{\alpha\alpha' r} B_r^\sigma(\alpha, \alpha') \mathbf{P}_r^\sigma(\alpha) \cdot \mathbf{P}_r^\sigma(\alpha') \end{aligned} \tag{2.5b}$$

$$\mathbf{H}^{\pi\nu} = \sum_{\varphi\varphi'} B_0^{\pi\nu}(\varphi, \varphi') \mathbf{N}_\varphi^\pi \mathbf{N}_{\varphi'}^\nu + \sum_{\alpha\alpha' r} B_r^{\pi\nu}(\alpha, \alpha') \mathbf{P}_r^\pi(\alpha) \mathbf{P}_r^\nu(\alpha'). \tag{2.5c}$$

In Eq. (2.5), $\sigma = \pi, \nu$ denotes protons or neutrons, respectively; e_j^σ is the spherical shell model single-particle energy and \mathbf{n}_j^σ is the corresponding number operator; $\mathbf{N}_\varphi^\sigma$ is the pair number operator, the index φ (φ') denotes normal ($\varphi = 1$) or abnormal-parity ($\varphi = 0$) levels; the ranks of multipole operators are $r = 1, 2$ for Sp_6 , and $r = 1, 2, 3$ for SO_8 cases. For index a ($a' = a$ or ba) denotes the multipole operators coupled from the active part defined in Eq. (2.3) ($a = k = 1$ for k -active and $a = i = 3/2$ for i -active); b denotes the multipole operators associated with broken pairs or unpaired particles, which are defined in Eq. (2.4).

The unpaired particles could in principle have multipole operators with $r > 2$ (3) for the Sp_6 (SO_8) case. The reason we do not consider those terms is that it is commonly thought to be that the higher order terms in a multipole expansion

of the effective interaction are less important since pairing has already taken care of the major part of the short range correlations. Furthermore, because of their single-particle nature, the strength of the multipole moment of unpaired particles should be much smaller than the collective ones; in addition, there is no coupling term between the collective 'core' and unpaired particles for $r > 2$ (3), because the highest order of collective multipole operators is $r = 2$ (3) for the Sp_6 (SO_8) symmetry.

The FDSM effective Hamiltonian Eq. (2.5) can be simplified through the following considerations. First, the single particle energy term can be rewritten in terms of the k - i basis

$$\sum_j e_j^\sigma \mathbf{n}_j^\sigma = \sum_{\lambda i} \Delta e_{\lambda i}^\sigma \mathbf{n}_{\lambda i}^\sigma + e_0^\sigma \mathbf{n}_0^\sigma + e_1^\sigma \mathbf{n}_1^\sigma \quad (2.6a)$$

with

$$\Delta e_{\lambda i}^\sigma = \sum_{j \in i} e_j^\sigma \begin{bmatrix} k & i & j \\ k & i & j \\ \lambda & \lambda & 0 \end{bmatrix} \sqrt{\Omega_j / \Omega_{ki}} - e_1^\sigma \quad (2.6b)$$

$$e_1^\sigma = \sum_{j \in i} e_j^\sigma \Omega_j / \Omega_1 \quad (2.6c)$$

$$\mathbf{n}_{\lambda i}^\sigma = \sqrt{2\Omega_{ki}} [\mathbf{b}_{ki}^{\sigma\dagger} \tilde{\mathbf{b}}_{ki}^\sigma]^{(\lambda\lambda)0} \quad (2.6d)$$

where $e_0^\sigma \equiv e_{j_0}^\sigma$ is the single-particle energy of the abnormal-parity level; e_1^σ is the average single-particle energy of the normal-parity levels; and $\sum \Delta e_{\lambda i}^\sigma \mathbf{n}_{\lambda i}^\sigma$ represents the effect of the normal-parity single-particle energy splitting. Notice that this term is nonzero only when there are unpaired particles (non-zero heritage $u \neq 0$); this explains why the FDSM can describe the low-lying structure of even-even nuclei reasonably well without considering the details of the single-particle splitting. However, for high-spin states or odd nuclei this term may have to be taken into account.

Second, assuming that the valence shells possess Sp_6 symmetry, the pairing energy terms can be rewritten in terms of SU_2 Casimir operator $C_{SU_2}^\sigma$ and $C_{su_2}^\sigma$, and the Sp_6 Casimir operator C_{sp_6} , by using the following relations:

$$C_{su_2}^\sigma = \mathbf{S}^{\sigma\dagger} \cdot \mathbf{S}^\sigma + S_0^\sigma (S_0^\sigma - 1), \quad S_0^\sigma = (n_0^\sigma - \Omega_0^\sigma) / 2 \quad (2.7a)$$

$$C_{SU_2}^\sigma = \mathbf{S}^{\sigma\dagger} \cdot \mathbf{S}^\sigma + \mathbf{S}_0^\sigma (\mathbf{S}_0^\sigma - 1), \quad \mathbf{S}_0^\sigma = (\mathbf{n}_1^\sigma - \Omega_1^\sigma) / 2 \quad (2.7b)$$

$$C_{sp_6}^\sigma = \mathbf{S}^{\sigma\dagger} \cdot \mathbf{S}^\sigma + \mathbf{D}^{\sigma\dagger} \cdot \mathbf{D}^\sigma + \sum_r \mathbf{P}_r^\sigma(k) \cdot \mathbf{P}_r^\sigma(k) + \mathbf{S}_0^\sigma (\mathbf{S}_0^\sigma - 6). \quad (2.7c)$$

Here, for simplicity, we drop the index φ and use \mathbf{S}^σ for \mathbf{S}^σ ($\varphi = 1$) (normal-parity level) and special characters S^σ , n_0^σ , etc., for abnormal-parity levels ($\varphi = 0$). Using

Eqs. (2.6) and (2.7), the first four terms in right side of Eq. (2.5b), denoted as \mathbf{H}_0^σ , can be rearranged in the following form

$$\mathbf{H}_0^\sigma = \sum_{\lambda i} \Delta e_{\lambda i}^\sigma \mathbf{n}_{\lambda i}^\sigma + \bar{\mathbf{H}}_0^\sigma + \mathbf{V}_P^\sigma \quad (2.8a)$$

$$\bar{\mathbf{H}}_0^\sigma = \varepsilon_0^\sigma \mathbf{n}_0^\sigma + \varepsilon_1^\sigma \mathbf{n}_1^\sigma + \nu_0 \mathbf{n}_0^\sigma (\mathbf{n}_0^\sigma - 1)/2 + \nu_1 \mathbf{n}_1^\sigma (\mathbf{n}_1^\sigma - 1)/2 + \nu_{10} \mathbf{n}_1^\sigma \mathbf{n}_0^\sigma \quad (2.8b)$$

$$\mathbf{V}_P^\sigma = G_2^\sigma \Delta \mathbf{C}_{sp6}^\sigma + \mathcal{G}_0^\sigma \Delta \mathbf{C}_{su2}^\sigma + (G_0^\sigma - G_2^\sigma) \Delta \mathbf{C}_{SU2}^\sigma + g_0^\sigma (\mathbf{S}^\dagger \cdot \mathbf{S}^{\sigma+} + \mathbf{S}^{\sigma\dagger} \cdot \mathbf{S}^\sigma) \quad (2.8c)$$

with

$$\Delta \mathbf{C}_{su2}^\sigma = \mathbf{C}_{su2}^\sigma - \Omega_0 (\Omega_0 + 2)/4 \quad (2.9a)$$

$$\Delta \mathbf{C}_{SU2}^\sigma = \mathbf{C}_{SU2}^\sigma - \Omega_1 (\Omega_1 + 2)/4 \quad (2.9b)$$

$$\Delta \mathbf{C}_{sp6}^\sigma = \mathbf{C}_{sp6}^\sigma - \Omega_1 (\Omega_1 + 12)/4 \quad (2.9c)$$

and

$$\varepsilon_0^\sigma = e_0^\sigma + \mathcal{B}_0^\sigma/4 + \mathcal{G}_0^\sigma (2\Omega_0 + 1)/4, \quad \varepsilon_1^\sigma = e_1^\sigma + B_0^\sigma/4 + G_0^\sigma (2\Omega_0 + 1)/4 \quad (2.9d)$$

$$\nu_0^\sigma = (\mathcal{B}_0^\sigma - \mathcal{G}_0^\sigma)/2, \quad \nu_1^\sigma = (B_0^\sigma - G_0^\sigma)/2, \quad \nu_{10}^\sigma = b_0^\sigma/2. \quad (2.9e)$$

The term $\bar{\mathbf{H}}_0^\sigma$ in Eq. (2.8a), can be interpreted as an average Hamiltonian: ε_0^σ and ε_1^σ are the average single particle energies, and ν_0 , ν_1 , ν_{10} are the average two-body interactions of abnormal-abnormal, normal-normal, and normal-abnormal orbits, respectively. Therefore $\bar{\mathbf{H}}_0^\sigma$ should be the leading term for the nuclear binding energy, and the particle number distribution among normal- and abnormal-parity levels should be determined mainly by this term. By making use of $N^\sigma = N_1^\sigma + N_0^\sigma$, $\bar{\mathbf{H}}_0^\sigma$ can be rewritten in the following form:

$$\bar{\mathbf{H}}_0^\sigma = A^\sigma (\mathbf{N}_1^\sigma)^2 - 2B^\sigma \mathbf{N}_1^\sigma + C^\sigma \quad (2.10a)$$

with

$$A^\sigma = 2(\nu_0^\sigma + \nu_1^\sigma - 2\nu_{10}^\sigma) \quad (2.10b)$$

$$B^\sigma = [\Delta \varepsilon_0^\sigma - (\nu_0^\sigma - \nu_{10}^\sigma)]/2 + 2(\nu_0^\sigma - \nu_{10}^\sigma) N^\sigma, \quad \Delta \varepsilon^\sigma = (\varepsilon_0^\sigma - \varepsilon_1^\sigma) \quad (2.10c)$$

$$C^\sigma = (\varepsilon_0^\sigma - \nu_{10}^\sigma/2)n^\sigma + (\nu_{10}^\sigma/2)(n^\sigma)^2. \quad (2.10d)$$

Imposing the energy minimization condition $\partial \bar{\mathbf{H}}_0^\sigma / \partial \mathbf{N}_1^\sigma = 0$, this leads to the following particle-number distribution

$$\mathbf{N}_1^\sigma = B^\sigma / A^\sigma = a^\sigma + b^\sigma N^\sigma \quad (2.11a)$$

where

$$a^\sigma = \frac{[\Delta\varepsilon^\sigma - (\nu_0^\sigma - \nu_1^\sigma)/2]}{2(\nu_0^\sigma + \nu_1^\sigma - 2\nu_{10}^\sigma)}, \quad b^\sigma = \frac{2(\nu_0^\sigma - \nu_{10}^\sigma)}{2(\nu_0^\sigma + \nu_1^\sigma - 2\nu_{10}^\sigma)}. \quad (2.11b)$$

Empirically we know that $N_1^\sigma \approx 0.75 + 0.5N^\sigma$ for $\sigma = \pi$ or ν (which can be obtained from Eq. (2.11) by assuming $\nu_0^\sigma = \nu_1^\sigma$ and $\Delta\varepsilon^\sigma/4(\nu_1^\sigma - \nu_{10}^\sigma) = 0.75$) is a good approximation for the ground state particle-number distribution in actinide and rare-earth nuclei^{2,9}). This suggests that the n - p monopole-monopole interaction term ($N_\phi^\pi N_\phi^\nu$) must be mainly of ($N^\pi N^\nu$) type so that it will not affect N_1^σ very much; this reduces the first sum on the right side of Eq. (2.5c) to just one term, $B_0^{\pi\nu} N^\pi N^\nu$.

Third, we may simplify the multipole-multipole interactions in Eq. (2.5) by assuming that they mainly depend on the collective quadrupole moment \mathbf{P}_2^σ , the total quadrupole moment of the unpaired particles \mathbf{q}_2^σ , the collective angular momentum \mathbf{R}^σ , and the total angular momentum of the unpaired particles \mathbf{I}^σ .

Thus,

$$\begin{aligned} \sum_{\alpha\alpha'} B_r^\sigma(a, \alpha') \mathbf{P}_r^\sigma(a) \cdot \mathbf{P}_r^\sigma(\alpha') &= B_2^\sigma \mathbf{P}_2^\sigma \cdot \mathbf{P}_2^\sigma - \chi^\sigma \mathbf{P}_2^\sigma \cdot \mathbf{q}_2^\sigma + \varkappa^\sigma \mathbf{q}_2^\sigma \cdot \mathbf{q}_2^\sigma + \\ &+ \alpha^\sigma \mathbf{R}^\sigma \cdot \mathbf{R}^\sigma + \delta^\sigma \mathbf{R}^\sigma \cdot \mathbf{I}^\sigma + \gamma^\sigma \mathbf{I}^\sigma \cdot \mathbf{I}^\sigma \end{aligned} \quad (2.12)$$

$$\begin{aligned} \sum_{\alpha\alpha'} B_r^{\pi\nu}(a, \alpha') \mathbf{P}_r^\pi(a) \cdot \mathbf{P}_r^\nu(\alpha') &= 2B_2^{\pi\nu} \mathbf{P}_2^\pi \cdot \mathbf{P}_2^\nu - \chi^{\pi\nu} \mathbf{P}_2^\pi \cdot \mathbf{q}_2^\nu - \\ - \chi^{\nu\pi} \mathbf{P}_2^\nu \cdot \mathbf{q}_2^\pi + 2\varkappa^{\pi\nu} \mathbf{q}_2^\pi \cdot \mathbf{q}_2^\nu + 2\alpha^{\pi\nu} \mathbf{R}^\pi \cdot \mathbf{R}^\nu + \delta^{\pi\nu} \mathbf{R}^\pi \mathbf{I}^\nu + \delta^{\nu\pi} \mathbf{R}^\nu \cdot \mathbf{I}^\pi + 2\gamma^{\pi\nu} \mathbf{I}^\pi \cdot \mathbf{I}^\nu. \end{aligned} \quad (2.13)$$

The relation between the angular momentum operators and the dipole operators $\mathbf{P}_1^\sigma(k)$ and $\mathbf{P}_1^\sigma(i)$ is known^{2,3}):

$$\mathbf{R}^\sigma = \sqrt{8/3} \mathbf{P}_1^\sigma(k), \quad \mathbf{I}^\sigma(i) = \sqrt{4i(i+1)/3} \mathbf{P}_1^\sigma(i) \quad (2.14a)$$

$$\mathbf{I} = \sum_i \mathbf{I}^\sigma(i), \quad \mathbf{J}^\sigma = \mathbf{R}^\sigma + \mathbf{I}^\sigma \quad (2.14b)$$

where \mathbf{J}^σ is the total angular momentum of protons ($\sigma = \pi$) or neutrons ($\sigma = \nu$).

The relation between the quadrupole moment operators and the quadrupole operators $\mathbf{P}_2^\sigma(k)$ and $\mathbf{P}_2^\sigma(b)$ can be found through a comparison with the original shell model quadrupole operator $Y_{2\mu}(\Theta, \varphi)$. The second-quantized form of the $Y_{2\mu}(\Theta, \varphi)$ operator in the k - i basis is

$$\begin{aligned}
 Y_{2\mu}(\Theta, \varphi) &= \sum_{KIj_1j_2} \frac{\langle j_1 || Y_2 || j_2 \rangle}{\sqrt{5}} \begin{bmatrix} k & i_1 & j_1 \\ k & i_2 & j_2 \\ K & I & 2 \end{bmatrix} [\mathbf{b}_{ki_1}^{\sigma\dagger} \tilde{\mathbf{b}}_{ki_2}^{\sigma}]_{\mu}^{(K)2} = \\
 &= \sum c(k, i) [\mathbf{b}_{ki}^{\sigma\dagger} \tilde{\mathbf{b}}_{ki}^{\sigma}]_{\mu}^{(20)2} + \sum_b c(b) \mathbf{P}_{2\mu}^{\sigma}(b)
 \end{aligned} \quad (2.15a)$$

where

$$c(k, i) = \sum_{j_1j_2i} \frac{\langle j_1 || Y_2 || j_2 \rangle}{\sqrt{5}} \begin{bmatrix} k & i & j_1 \\ k & i & j_2 \\ 2 & 0 & 2 \end{bmatrix} \quad (2.15b)$$

$$c(b) = \sum_{i_1j_2cb} \frac{\langle j_1 || Y_2 || j_2 \rangle}{\sqrt{5}} \begin{bmatrix} k & i_1 & j_1 \\ k & i_2 & j_2 \\ K & I & 2 \end{bmatrix}. \quad (2.15c)$$

In the FDSM, $\mathbf{P}_2^{\sigma}(k)$ is assumed to be proportional to the collective quadrupole moment $\mathbf{Q}_2^{\sigma} = a\mathbf{P}_2^{\sigma}$, where $\mathbf{P}_2^{\sigma} \equiv -\mathbf{P}_2^{\sigma}(k)$. The negative sign is for convenience so that the constant a will be a positive number and $e_{eff} = a \times e$ or $m_{eff} = a \times m$ may be interpreted as an effective charge or effective mass for the electric-quadrupole moment or mass quadrupole moment, respectively. The total quadrupole moment is then the sum of the collective quadrupole moment \mathbf{Q}_2^{σ} , and the total quadrupole moment of the unpaired particles \mathbf{q}_2^{σ} :

$$\mathbf{Q}_2^{\sigma} = \mathbf{Q}_2^{\sigma} + \mathbf{q}_2^{\sigma} \quad (2.16a)$$

and

$$\mathbf{Q}_{2\mu}^{\sigma} = a\mathbf{P}_{2\mu}^{\sigma} = -a \sum_i \sqrt{\Omega_{ki}^{\sigma}}/2 [\mathbf{b}_{ki}^{\sigma\dagger} \tilde{\mathbf{b}}_{ki}^{\sigma}]_{\mu}^{20}. \quad (2.16b)$$

Upon comparing Eq. (2.16) and the shell model expression (2.15), it is clear that the collective quadrupole moment $\mathbf{Q}_{2\mu}^{\sigma}$ corresponds to the first term on the right side of Eq. (2.15a), but with the coefficients $c(k, i)$ replaced by $-a(\Omega_{ki}^{\sigma}/2)^{1/2}$, which may be interpreted as a kind of renormalization. This is understandable; since our space is highly truncated, the operator must be renormalized to effectively include the contributions from the configurations which lie outside of the model space. Therefore, our collective quadrupole operator should not be the same as the ordinary shell model one. The collective quadrupole moment $\mathbf{Q}_{2\mu}^{\sigma}$, after renormalization, should be much larger than its corresponding shell model part without renormalization. However, the renormalization of the quadrupole moment of the unpaired particles, which is basically of single-particle nature, should not be very large. It may be a good approximation to assume that \mathbf{q}_2^{σ} is simply the second term of Eq. (2.15a), without renormalization:

$$\mathbf{q}_2^{\sigma} = \sum_b c(b) \mathbf{P}_{2\mu}^{\sigma}(b). \quad (2.17)$$

Thus the FDSM Hamiltonian can be regrouped into four terms:

$$\mathbf{H}_{FSD} = \mathbf{H}_0 + \mathbf{V}_p + \mathbf{H}_{c0} + \mathbf{H}_{pc} \quad (2.18a)$$

$$\mathbf{H}_0 = \sum_{\sigma ki} \Delta e_{ki}^{\sigma} \mathbf{n}_{ki} + \overline{\mathbf{H}}_0^{\pi} + \overline{\mathbf{H}}_0^{\nu} + B_0^{\pi\nu} \mathbf{N}^{\pi} \mathbf{N}^{\nu} \quad (2.18b)$$

$$\begin{aligned} \mathbf{V}_p = \sum_{\sigma} \{ & G_2^{\sigma} \Delta \mathbf{C}_{sp6}^{\sigma} + \mathcal{G}_0^{\sigma} \Delta \mathbf{C}_{su2}^{\sigma} + (G_0^{\sigma} - G_2^{\sigma}) \Delta \mathbf{C}_{SU2}^{\sigma} + \\ & + g_0^{\sigma} (\mathbf{S}^{\sigma\dagger} \cdot \mathbf{S}^{\sigma} + \mathbf{S}^{\sigma\dagger} \cdot \mathbf{S}^{\sigma}) \} \end{aligned} \quad (2.18c)$$

$$\mathbf{H}_{c0} = \sum_{\sigma\sigma'} \{ (B_2^{\sigma\sigma'} - G_2^{\sigma} \delta_{\sigma\sigma'}) \mathbf{P}_2^{\sigma} \cdot \mathbf{P}_2^{\sigma'} + \alpha^{\sigma\sigma'} \mathbf{R}^{\sigma} \cdot \mathbf{R}^{\sigma'} \} \quad (2.18d)$$

$$\mathbf{H}_{pc} = \sum_{\sigma\sigma'} \{ -\chi^{\sigma\sigma'} \mathbf{P}_2^{\sigma} \cdot \mathbf{q}_2^{\sigma'} + \kappa^{\sigma\sigma'} \mathbf{q}_2^{\sigma} \cdot \mathbf{q}_2^{\sigma'} + \delta^{\sigma\sigma'} \mathbf{R}^{\sigma} \cdot \mathbf{I}^{\sigma'} + \gamma^{\sigma\sigma'} \mathbf{I}^{\sigma} \cdot \mathbf{I}^{\sigma'} \}. \quad (2.18e)$$

In Eq. (2.18) each term has a clear physical meaning: the first term \mathbf{H}_0 depends only on the number distribution of valence nucleons; the second term \mathbf{V}_p is the pairing (including quadrupole pairing) excitation energy; the third term describes collective motion; and the last term describes the motion of unpaired particles, and their coupling with the collective motion. In Eq. (2.18d) the strength of $\mathbf{P}_2^{\sigma} \cdot \mathbf{P}_2^{\sigma'}$ changes from $B_2^{\sigma\sigma'}$ to $(B_2^{\sigma\sigma'} - G_2^{\sigma} \delta_{\sigma\sigma'})$ by virtue of the transformation of (2.7c) when we convert the quadrupole pairing term into $\mathbf{C}_{sp6}^{\sigma}$.

If a strong n-p interaction is assumed so that the nuclear collective motion mainly depends on the total quadrupole moments $\mathbf{P}_{\mu}^2 = \mathbf{P}_{2\mu}^{\nu} + \mathbf{P}_{2\mu}^{\pi}$ and $\mathbf{q}_{\mu}^2 = \mathbf{q}_{2\mu}^{\nu} + \mathbf{q}_{2\mu}^{\pi}$, and the total angular momenta, $\mathbf{R} = \mathbf{R}^{\pi} + \mathbf{R}^{\nu}$ and $\mathbf{I} = \mathbf{I}^{\pi} + \mathbf{I}^{\nu}$, rather than proton and neutron ones separately, the FDSM Hamiltonian is simplified to

$$\begin{aligned} \mathbf{H}_{FSD} = & \mathbf{H}_0 + \mathbf{V}_p + \alpha \mathbf{R}^2 - \chi \mathbf{P}^2 \cdot \mathbf{q}^2 + \delta \mathbf{R} \cdot \mathbf{I} + \kappa \mathbf{q}^2 \cdot \mathbf{q}^2 + \gamma \mathbf{I}^2 + \\ & + B_2^{\pi\nu} \mathbf{C}_{su3}^{\pi+\nu} + (B_2^{\pi} - G_2^{\pi} - B_2^{\pi\nu}) \mathbf{C}_{su3}^{\pi} + (B_2^{\nu} - G_2^{\nu} - B_2^{\pi\nu}) \mathbf{C}_{su3}^{\nu} \end{aligned} \quad (2.19)$$

where $\mathbf{C}_{su3}^{\pi+\nu}$ and $\mathbf{C}_{su3}^{\sigma}$ are the Casimir operators of $SU_3^{\pi+\nu}$ and SU_3^{σ} , respectively,

$$\mathbf{C}_{su3}^{\pi+\nu} = \mathbf{P}^2 \cdot \mathbf{P}^2 + \mathbf{P}^1 \cdot \mathbf{P}^1, \quad \mathbf{C}_{su3}^{\sigma} = \mathbf{P}_2^{\sigma} \cdot \mathbf{P}_2^{\sigma} + \mathbf{P}_1^{\sigma} \cdot \mathbf{P}_1^{\sigma}; \quad (2.20)$$

There are many other possibilities for further reducing the number of parameters which depend on physical considerations. For example, the first two terms in Eq. (2.18c) only depend on the highest symmetry $Sp_6 \times SU_2$ which is characterized by the the heritage number $u = u_1 + \nu_0$, the sum of the number of unpaired particles in normal-parity levels (u_1) and the abnormal-parity levels (ν_0).

For no unpaired particles ($u = 0$), these terms are zero; therefore they may be regarded as the excitation energy for unpaired particles. For a given u , these two terms just provide a constant. The last term in Eq. (2.18c) is the pairing correlation between normal and abnormal-parity levels. This term has vanishing diagonal matrix elements, and may be neglected in the case where the quadrupole interaction becomes dominant. If we believe that the quadrupole-quadrupole interactions among like particle are small (which is a conjecture with considerable empirical support), these terms may be neglected and the FDSM Hamiltonian can be simplified as

$$\begin{aligned} \mathbf{H}_{FSD} = \mathbf{H}_0 + \mathbf{V}_p + B_2^{n\nu} \mathbf{C}_{iu_3}^{n+\nu} + \alpha \mathbf{R}^2 - \chi \mathbf{P}^2 \cdot \mathbf{q}^2 + \\ + \delta \mathbf{R} \cdot \mathbf{I} + \kappa \mathbf{q}^2 \cdot \mathbf{q}^2 + \gamma \mathbf{I}^2. \end{aligned} \quad (2.21)$$

For even-even nuclei with no broken pairs ($u = 0$), this reduces to just

$$\mathbf{H}_{FDS} = \mathbf{H}_0 + \sum_{\sigma} (G_0^{\sigma} - G_2^{\sigma}) \Delta C_{SU_2}^{\sigma} + B_2^{n\nu} \mathbf{C}_{iu_3}^{n+\nu} + \alpha \mathbf{R}^2 \quad (2.22)$$

where H_0 is a constant depending only on the number distribution since $\sum \Delta e_{\lambda i}^{\sigma} n_{\lambda i}^{\sigma}$ acting on the $u = 0$ space is zero. In this approximation only 4 parameters are required for describing low lying collective modes!

Of course we do not really know yet what the detailed FDSM effective interactions should be. What we have discussed so far are just some plausible effective interactions within the FDSM framework. In order to determine the complete FDSM effective interaction a systematic analysis is required to see whether a set of parameters can be obtained to fit all the known data consistently for nuclei in a certain region, just as was done for the shell model in s-d shell nuclei. Because of the very nice regularity of the low lying properties of heavy nuclei, we may surmise that the relevant parameters which are responsible for low lying nuclear structure should be limited in number. The question has been how to find them. The FDSM seems to provide a practical way to carry this out.

3. The particle-rotor model and the FDSM

Let us consider a system with n_0 unpaired particles in the abnormal-parity level and $N_1 = (n_1/2)$ pairs in the normal parity levels. In the particle-rotor model (PRM), this system is usually treated as a rotating «core» plus n_0 individual particles moving in the deformed potential generated by the «core». The Hamiltonian is

$$\mathbf{H}_{PR} = \sum_{\sigma} \varepsilon_0^{\sigma} n_0^{\sigma} - \sum_{i=1}^{n_0} \beta m \omega_i^2 r_i'^2 Y_{20}(\Theta_i') + \frac{\mathbf{R}^2}{2\mathcal{I}} + \mathbf{H}_{vib}(\beta, \gamma). \quad (3.1)$$

It contains the spherical single-particle energy of the individual particles $\varepsilon_0^{\sigma} n_0^{\sigma}$, the Nilsson deformed potential $\beta m \omega_0^2 r_i'^2 Y_{20}(\Theta_i')$, the rotational energy of the core $\mathbf{R}^2/2\mathcal{I}$, and the β - γ vibrational energy $\mathbf{H}_{vib}(\beta, \gamma)$. The symbols r_i' Θ_i' are the coor-

dinates of particles in a body-fixed frame. In the FDSM the simplified $Sp_6^7 \times Sp_6^7$ Hamiltonian shown in (2.21) has very similar behaviour. In Eq. (3.1) the ground state energy of the even core is taken as the energy zero point, pairing is not included for simplicity, the interactions among the n_0 particles are neglected, and no spin-spin coupling between the core and particles is considered. For comparison purposes we neglect the corresponding terms in the FDSM Hamiltonian and subtract the constant part of \mathbf{H}_0 , together with the expectation value of the SU_3 Casimir operator of the ground state (which corresponds to the ground state energy of the even core). Eq. (2.21) becomes

$$\mathbf{H}_{FDS} = \sum_{\sigma} \varepsilon_0^{\sigma} \mathbf{n}_0^{\sigma} - \chi \mathbf{P}^2 \cdot \mathbf{q}^2 + \alpha \mathbf{R}^2 + B_2 \Delta C_{su3}^{\pi+\nu} \quad (3.2)$$

where $B_2 = |B_2^{\pi\nu}|$, and

$$\Delta C_{su3}^{\pi+\nu} = C_{su3}^{\pi+\nu}(n_1, 0) - C_{su3}^{\pi+\nu}(\lambda, \mu) \quad (3.3)$$

is the difference of the expectation values of the SU_3 Casimir operators in the (λ, μ) representation and the ground state representation $(n_1, 0)$. In the $SU_3^{\pi+\nu}$ limit the expectation values of the Casimir operators are known:

$$C_{su3}^{\pi+\nu}(\lambda, \mu) = (\lambda^2 + \mu^2 + \lambda\mu + 3\lambda + 3\mu)/2, \quad C_{su3}^{\pi+\nu}(n_1, 0) = n_1(n_1 + 3)/2. \quad (3.4)$$

A comparison of the Hamiltonians (3.1) and (3.2) is shown in Table 3.

From Table 3, one can see very clearly that there is a one to one correspondence between these two model Hamiltonians. In the FDSM the quadrupole-quadrupole interactions between unpaired particles in the abnormal level and the S - D pairs in normal-parity levels $-\chi \mathbf{P}^2 \mathbf{q}^2$ play the same role as the Nilsson deformed potential in the PRM. The S - D pairs form the »deformed core« and its rotational energy $\alpha \mathbf{R}^2$ corresponds to the rotor Hamiltonian $\mathbf{R}^2/2\theta$.

Furthermore, if the weak-coupling basis is used for the PRM

$$|(n_{\beta}, n_{\nu}) RK(j_0)^{n_0} \sigma I JM\rangle = \sum_{m\mu} \chi_{n_{\beta} n_{\nu}}(\beta, \gamma) \mathcal{D}_{mK}^R(\Omega) \varphi_{\mu}^{\sigma I}(\mathbf{r}_i) C_{RMj\mu}^{JM} \quad (3.5)$$

where $\chi_{n_{\beta} n_{\nu}}(\beta, \gamma)$ is the eigenfunction of $\mathbf{H}_{vib}(\beta, \gamma)$, $\mathcal{D}_{mK}^R(\Omega)$ is the rotor eigenfunction, and $\varphi_{\mu}^{\sigma I}(\mathbf{r}_i)$ is a basis for n_0 particles in the abnormal level, it can be shown that the difference between the matrix elements of PRM Hamiltonian \mathbf{H}_{PR} in this basis and the FDSM Hamiltonian \mathbf{H}_{FDS} in the SU_3 basis is of order $1/n_1$:

$$\begin{aligned} &\langle (n_{\beta}, n_{\nu}) R' K' (j_0)^{n_0} \sigma' I' ; JM | \mathbf{H}_{PR} | (n_{\beta}, n_{\nu}) RK(j_0)^{n_0} \sigma I ; JM \rangle = \\ &= \langle (\lambda, \mu) R' \kappa' (j_0)^{n_0} \sigma' I' ; JM | \mathbf{H}_{FDS} | (\lambda, \mu) \cdot R\kappa(j_0)^{n_0} \sigma j ; JM \rangle + O(1/n_1). \end{aligned} \quad (3.6)$$

Thus in large n_1 limit ($n_1 \rightarrow \infty$), these two models become identical.

To prove this the key point is to demonstrate that

$$\begin{aligned} & \langle (\lambda, \mu) R' \kappa' (j_0)^{n_0} \sigma' I'; JM | \chi \mathbf{P}^2 \cdot \mathbf{q}^2 | (\lambda, \mu) R \kappa (j_0)^{n_0} \sigma j; JM \rangle = \\ & = \langle (n_\beta, n_\gamma) R' K' (j_0)^{n_0} \sigma' I'; JM | \sum_{i=1}^{n_0} \beta r_i'^2 m \omega_i^2 Y_{20}(\Theta_i') | (n_\beta, n_\gamma) \cdot \\ & \quad \cdot RK(j_0)^{n_0} \sigma I; JM \rangle + O(1/n_1) \end{aligned} \tag{3.7}$$

and

$$B_2^{\pi\lambda} \Delta C_{su3}^{\pi+\nu} = \hbar\omega (n_\gamma + n_\beta + K/2) + O(1/n_1) \tag{3.8}$$

TABLE 3.

The PRM		The FDSM	
Hamiltonian	$\mathbf{H}_{PRR} =$	$\mathbf{H}_{FDS} =$	Hamiltonian
S. P. Energy	$\sum_{\sigma} \varepsilon_{\sigma}^{\alpha} n_{\sigma}^{\alpha}$	$\sum_{\sigma} \varepsilon_{\sigma}^{\alpha} n_{\sigma}^{\alpha}$	S. P. Energy
Deformed Potential	$-\sum_{i=1}^{n_0} \beta r_i'^2 m \omega_0^2 Y_{20}(\Theta_i')$	$-\chi \mathbf{P}^2 \cdot \mathbf{q}^2$	$Q \cdot Q$ Coupling
Core Rotation	$+\frac{\mathbf{R}^2}{2\theta}$	$+a\mathbf{R}^2$	S-D pair Rotation
$\beta - \gamma$ vibration	$+\mathbf{H}_{vib}(\beta, \gamma)$	$+B_2^{\pi\nu} \Delta C_{su3}^{\pi+\nu}$	SU_3 Casimir
	* * * * *	* * * * *	
r_i', Θ_i' defined in the Body-fix Frame		\mathbf{H}_{FSD} defined in the Laboratory Frame	
PRM Weak-Coupling Basis:		FDSM SU_3 Basis:	
$ (n_\beta, n_\gamma) RK(j_0)^{n_0} \sigma j; JM\rangle$		$ (\lambda, \mu) R \kappa (j_0)^{n_0} \sigma j; JM\rangle$	
$= \sum_{m\mu} \chi(n_\beta, n_\gamma) \mathcal{D}_{mK}^R(\Omega) \varphi_{\mu}^{\sigma I}(r_i) C_{RM I \mu}^{JM}$		$= \sum_{m\mu} (\lambda, \mu) R \kappa (j_0)^{n_0} \sigma j; JM\rangle \varphi_{\mu}^{\sigma I}(r_i) C_{RM I \mu}^{JM}$	

A comparison between the Particle-Rotor Model and the FDSM.

where $\hbar\omega (n_\gamma + n_\beta + K/2)$ is the eigenvalue of the β - γ vibration energy $\mathbf{H}_{vib}(\beta, \gamma)$. The other terms in Eq. (3.1) and (3.2) are the same, as shown in Table 3, if we identify $a = 1/2\theta$.

To demonstrate Eq. (3.7), one first should transfer $Y_{20}(\Theta_i')$ from the body-fixed frame to the laboratory frame:

$$Y_{20}(\Theta_i') = Y_2(\Omega) \cdot Y_2(\Theta_{ib}, \varphi_i). \tag{3.9}$$

Then one can obtain

$$\begin{aligned} & \langle (n_\beta, n_\gamma) R' K' (j_0)^{n_0} \sigma' I'; JM | \sum_{i=1}^{n_0} \beta r_i'^2 m \omega_i^2 Y_{20}(\Theta_i) | (n_\beta, n_\gamma) RK \cdot \\ & \cdot (j_0)^{n_0} \sigma I; JM \rangle = \beta \langle r^2 \rangle m \omega_0^2 U(R 2 J I'; R' I) \sqrt{\frac{2R+1}{2R'+1}} C_{RK'20}^{R'K'} \times \\ & \times \frac{1}{\sqrt{2I+1}} \langle (j_0)^{n_0} \sigma' I' || \sum_{i=1}^{n_0} Y_2(\Theta_i, \varphi_i) || (j_0)^{n_0} \sigma I \rangle \end{aligned} \quad (3.10)$$

where $\langle r^2 \rangle$ is the average of r_i^2 and $U(R 2 J I'; R' I)$ is a Racah coefficient. Note that the operator \mathbf{q}_μ^2 for abnormal levels is the second quantized form of $\sum Y_2(\Theta_i, \varphi_i)$: since $k = 0$, according to Eqs. (2.4), (2.5) and (2.17),

$$\mathbf{q}_{2\mu}^\sigma(j_0) = \frac{\langle j_0 | |Y_2| | j_0 \rangle}{\sqrt{5}} \begin{bmatrix} 0 & j_0 & j_0 \\ 0 & j_0 & j_0 \\ 0 & 2 & 2 \end{bmatrix} \mathbf{P}_{2\mu}^\sigma(j_0) = \frac{\langle j_0 | |Y_2| | j_0 \rangle}{\sqrt{5}} [\mathbf{b}_{j_0}^{\sigma\dagger} \tilde{\mathbf{b}}_{j_0}^\sigma]_{\mu}^2. \quad (3.11)$$

Thus, Eq. (3.10) can be written as

$$\begin{aligned} & \langle (n_\beta, n_\gamma) R' K' (j_0)^{n_0} \sigma' I'; JM | \sum_{i=1}^{n_0} \beta r_i'^2 m \omega_i^2 Y_{20}(\Theta_i) | (n_\beta, n_\gamma) RK \cdot (j_0)^{n_0} \sigma I; JM \rangle = \\ & = \beta \langle r^2 \rangle m \omega_0^2 U(R 2 J I'; R' I) \sqrt{\frac{2R+1}{2R'+1}} C_{RK'20}^{R'K'} \times \\ & \times \frac{1}{\sqrt{2I+1}} \langle (j_0)^{n_0} \sigma' I' || \mathbf{q}^2 || (j_0)^{n_0} \sigma I \rangle \end{aligned} \quad (3.12)$$

On the other hand,

$$\begin{aligned} & \langle (\lambda, \mu) \kappa' R' (j_0)^{n_0} \sigma' I'; JM | \chi \mathbf{P}^2 \cdot \mathbf{q}^2 | (\lambda, \mu) \kappa R (j_0)^{n_0} \sigma j; JM \rangle = \\ & = \chi U(R 2 J I'; R' I) \frac{1}{\sqrt{2R'+1}} \langle (\lambda, \mu) \kappa' R' || \mathbf{P}^2 || (\lambda, \mu) \kappa R \rangle \times \\ & \times \frac{1}{\sqrt{2I+1}} \langle (j_0)^{n_0} \sigma' I' || \mathbf{q}^2 || (j_0)^{n_0} \sigma I \rangle \end{aligned} \quad (3.13)$$

and

$$\begin{aligned} & \langle (\lambda, \mu) \kappa' R' || \mathbf{P}^2 || (\lambda, \mu) \kappa R \rangle = -(-1)^{\varphi(\mu)} \sqrt{C_{\mu 3}^{\lambda+\mu}(\lambda, \mu)} \times \\ & \times \langle (\lambda, \mu) \kappa R; (11) 2 || (\lambda, \mu) \kappa' R' \rangle \end{aligned} \quad (3.14a)$$

with

$$(-1)^{\varphi(\mu)} = \begin{cases} -1 & \text{if } \mu = 0 \\ 1 & \text{if } \mu \neq 0. \end{cases} \quad (3.14b)$$

It has been demonstrated by Elliott that (see Ref. 13, Eq. (45))

$$\langle (\lambda, \mu) \kappa' R' || \mathbf{P}^2 || (\lambda, \mu) \kappa R \rangle = \pm \sqrt{2R+1} (\lambda/\sqrt{2}) G_{R\kappa 20}^{R\kappa'} + O(1/\lambda) \\ \text{(for } \lambda \geq \mu \text{ and } \kappa) \quad (3.15)$$

(Note: Elliott's quadrupole operator \mathbf{Q} differs from \mathbf{P}^2 by a factor of $\sqrt{8}$). In Eq. (3.15), the $+(-)$ sign is for $n_1 \leq \Omega_1/2 (>\Omega_1/2)$, and for $n_1 > \Omega_1/2$, the hole (conjugate) representation is used. Thus in the large n_1 limit ($\lambda \approx n_1 \geq \mu$),

$$\langle (\lambda, \mu) \kappa' R' (j_0)^{n_0} \sigma' I'; JM | \chi \mathbf{P}^2 \cdot \mathbf{q}^2 | (\lambda, \mu) \kappa R (j_0)^{n_0} \sigma j; JM \rangle = \\ = \chi (n_1/\sqrt{2}) U(R 2 J I'; R' I) \sqrt{\frac{2R+1}{2R'+1}} G_{R\kappa 20}^{R\kappa'} \times \\ \times \frac{1}{\sqrt{2I+1}} \langle (j_0)^{n_0} \sigma' I' || \mathbf{q}^2 || (j_0)^{n_0} \sigma I \rangle + O(1/n_1). \quad (3.16)$$

Comparing Eq. (3.16) and (3.12), we see that Eq. (3.7) is valid provided we make the following identifications:

$$\beta = \frac{\chi/\sqrt{2}}{m\omega_0^2 \langle r^2 \rangle} n_1, \quad K = \kappa. \quad (3.17)$$

That is, the nuclear deformation β is proportional to n_1 , the number of nucleons in the normal-parity levels, and the Vergados quantum number¹³⁾ κ is equal to the angular momentum projection quantum number K .

Now, let us prove Eq. (3.8). As shown in Table 4, there is a one-to-one correspondence between each β - γ vibrational state classified by quantum numbers (n_β, n_γ, K) and an SU_3 representation classified by quantum numbers (λ, μ, K) :

$$n_\gamma = h_3 = (n_1 - \lambda - 2\mu)/3 \quad n_\beta = (\mu - \kappa)/2 \quad (3.18a)$$

$$\lambda = n_1 - 3n_\gamma - 4n_\beta - 2K \quad \mu = 2n_\beta + \kappa \quad (3.18b)$$

and one can convert SU_3 quantum numbers (λ, μ, κ) to β - γ vibrational quantum numbers (n_β, n_γ, K) or vice versa. It is very interesting to note that n_γ is nothing but h_3 , the number of particles in the third row of the U_3 Young diagram.

TABLE 4.

$E_{vib}(\beta, \gamma)$	$n_\gamma n_\beta k/2$	$h_3(\lambda, \mu) k$	$[h_1 h_2 h_3]$	$B_2 \Delta C(\lambda, \mu)$
0	0 0 0	$0(n_1, 0) 0$	$\overline{1 2 3 4 5 6 \dots n_1 }$	0
$\hbar\omega$	0 1 0 0 0 1	$0(n_1 - 4, 2) 0$ $0(n_1 - 4, 2) 2$	$\overline{1 2 3 4 5 6 \dots n_1 }$ $\dots n_1 $	$\hbar\omega \left(1 - \frac{1}{n_1}\right)$
$2\hbar\omega$	0 2 0 0 1 1 0 0 2	$0(n_1 - 8, 4) 0$ $0(n_1 - 8, 4) 2$ $0(n_1 - 8, 4) 4$	$\overline{1 2 3 4 5 6 \dots n_1 }$ $\dots \dots n_1 $	$2\hbar\omega \left(1 - \frac{3}{n_1}\right)$
	2 0 0	$2(n_1 - 6, 0) 0$	$\overline{1 2 3 4 5 6 \dots n_1 }$ $\dots \dots n_1 $	$2\hbar\omega \left(1 - \frac{3}{2n_1}\right)$
$3\hbar\omega$	0 3 0	$0(n_1 - 12, 6) 0$	$\overline{1 2 3 4 5 6 \dots n_1 }$	$3\hbar\omega \left(1 - \frac{5}{n_1}\right)$
	0 2 1	$0(n_1 - 12, 6) 2$	$\dots \dots \dots n_1 $	
	0 1 2	$0(n_1 - 12, 6) 4$	$\overline{1 2 3 4 5 6 \dots n_1 }$	$3\hbar\omega \left(1 - \frac{10}{3n_1}\right)$
	0 0 3	$0(n_1 - 12, 6) 6$	$\dots \dots \dots n_1 $	

$\beta - \gamma$ vibrations & SU_3 representations.

Using Eq. (3.18), it is easy to show that

$$B_2 \Delta C_{su3}^{2+\nu} = \hbar\omega (n_\gamma + n_\beta + K/2) \left\{ 1 - \frac{3n_\gamma(n_\gamma + \mu - 1) + \mu(\mu - 1)}{2n_1(n_\gamma + n_\beta + K/2)} \right\} \quad (3.19b)$$

$$\hbar\omega = 3B_2 n_1. \quad (3.19c)$$

In the large n_1 limit the anharmonic term vanishes and Eq. (3.19b) becomes identical to the GM result; thus Eq. (3.8) is justified. Having done this, we can finally conclude that the particle-rotor model is the large n_1 limit of the FDSM. One may even regard the foregoing as a shell-model derivation of the phenomenological particle-rotor model, since the parameters of the FDSM version of the particle-rotor model are functions of the FDSM effective interaction.

4. β - γ excitations and the dynamical Pauli effect

According to Eq. (3.19c) the FDSM predicts that the frequency of β - γ vibrations is proportional to the number of particles in the normal-parity valence

levels. It is very interesting to check whether this is consistent with experimental data. Since this result is for the SU_3 symmetry limit, the well deformed actinide nuclei are good candidates for this test: according to Table 2, for actinides both valence protons and neutrons possess Sp_6 symmetry and therefore can have an $SU_{3^{+\nu}}$ limit. (There are more data in the rare-earth region; unfortunately, the proton valence shell and neutron valence shell there possess different symmetries: the proton shell is SO_8 and the neutron shell is Sp_6 , and the situation is more complicated.)



Fig. 2. The band-head energies of the first β - and γ -band. Boxes are data taken from Ref. 14; lines are an FDSM fitting assuming the form of Eq. (3.19).

Fig. 2 shows the first β and γ -band band-head energies E_β and E_γ , for all well-deformed nuclei in the actinide region (heavier than ^{228}Th with $E4/E2 > 3.25$). One can see that they are indeed proportional to n_1 . The value $n_1 = 2N_1$ is determined by Eq. (2.11) with $a^\sigma = 0.75$ and $b^\sigma = 0.5$:

$$n_1^\sigma = 1.5 + 0.5n^\sigma \tag{4.1}$$

$$n_1 = n_1^\pi + n_1^\nu. \tag{4.2}$$

One of the most remarkable things about Fig. 2 is the sudden drop of the γ -band band-head when $n_1 > 24$, which is exactly what the FDSM expected. According to the FDSM the precondition for the excitation energy of the first γ -band to be one $\hbar\omega$ (disregarded the rotational energy for angular momentum 2) is that the ground band belongs to the totally symmetric $(n_1, 0)$ SU_3 representation. However,

this is true only when $n_1^0 \leq 2\Omega_1^0/3$. When $n_1^0 > 2\Omega_1^0/3$ the totally symmetric $(n_1, 0)$ representation is forbidden by the Pauli principle, and the ground band has to change from $(n_1, 0)$ to some other allowed representation with $\mu \neq 0$. Therefore, in the SU_3 limit a very low γ -band, which belongs to the same SU_3 representation as the ground band but has $K = 2$, will be expected. The excitation energy of the first γ -band in this case will suddenly drop from one $\hbar\omega$ to almost zero when $n_1^0 > 2\Omega_1^0/3$. This is very similar to what happens in the actinides! The critical number $n_1 = 24$ is just $2\Omega_1/3$ (Note that for actinides $\Omega_7^+ = 15$ and $\Omega_7^- = 21$; therefore $2\Omega_7^+/3 = 10$, $2\Omega_7^-/3 = 14$, and $2\Omega_1/3 = 24$). The drop of the dark boxes beyond $2\Omega_1/3$ is quite impressive, but there is even more: in fact, only one type of nucleon exceeding $2\Omega_1/3$ is enough to prohibit the $(n_1, 0)$ representation. In Fig. 1 the nuclei indicated by open boxes are those nuclei for which $n_1 < 2\Omega_1/3$, but which have neutron number $N = 152$ (corresponding to $n_1^0 = 14.5$, just exceeding $2\Omega_1/3$). For these nuclei E_γ also drops significantly. Although the drop for either the dark or open boxes is not as sharp as the pure SU_3 symmetry limit predicts, this can be explained by small n_1 configuration mixing due to symmetry breaking terms. Such mixing in the excited states is expected on quite general grounds.

In contrast, the first β -band behaves differently. When $n_1^0 > 2\Omega_1^0/3$ the first β -band should still go up linearly according to the FDSM, because it belongs to a higher representation and therefore the excitation energy can still be one $\hbar\omega$. Unfortunately, there are no data for $n_1 > 2\Omega_1/3$, but the β -band band-head for the two nuclei at the boundary with neutron number $N = 152$ (the open boxes) show no tendency to drop.

The dynamical Pauli effect is one of the most significant new discoveries of the FDSM. It is in fact a nature consequence of the SU_3 symmetry. Generally speaking, since U_3 is described by a three row Young diagram; the maximum number of particles which can be put in one row is one third of the shell degeneracy. Thus, for a system which possesses SU_3 symmetry, once one third of the shell is filled additional particles will have to go to the second row since there is no room in the first row because of the Pauli principle. The system then has to undergo a structural change, from a symmetric representation to a non-symmetric representation. Therefore, some sort of discontinuity in physical quantities may be expected. This effect has been found in several different places: the shell correction for actinide masses changes its behaviour at $N = 151$ and $Z = 99$ ⁸⁾; the $B(E2)$ and nuclear deformation become saturated at $N = 151$ and $Z = 99$ for actinides⁸⁾; the same saturation occurs at $N = 99$ for rare-earths but, as predicted by the FDSM, there is no saturation behaviour with respect to Z except for the ordinary particle-hole symmetry at $Z = 67$ (corresponding to $n_1^0 = \Omega_7^+ = 10$)⁹⁾. The sudden drop of the γ -band band-head at $N = 151$ and $Z = 99$ presented in this paper provides another piece of evidence for the dynamical Pauli effect. The critical number 151 and 99 are just the number of protons or neutrons at which the corresponding proton number or neutron number in the normal-parity levels reaches one third of the Sp_6 shells. For instance, in shell 7, 99 particles corresponds to 17 valence protons (neutrons) for actinides (rare-earths), implying 10 particles in the normal-parity levels according to Eq. (2.11), which is exactly $2\Omega_1/3$ of the shell (see Table 2); similarly, 151 particles corresponding to 25 valence nucleons, implying 14 particles in the normal-parity level of shell 8, which is again $2\Omega_1/3$ of this shell. On the other hand, shell 6 has SO_8 symmetry, which does not have an SU_3 subgroup; this explains why there is no $B(E2)$ saturation behaviour with respect to

proton number for rare-earth nuclei. Experimental data showing this discontinuity imply that heavy rotational nuclei do have rather good SU_3 symmetry. The appearance of structure changes at the critical numbers 99 and 152 is compelling evidence for the microscopic correctness of the FDSM SU_3 dynamical symmetry.

5. Summary

The equivalence of the FDSM and the PRM was first established in 1987¹⁵⁾ for the ground-band, and first β - and γ -band. Since then, a series of papers has studied the connections between the FDSM and GM to see how the FDSM, which has neither *deformations* nor *mean fields*, can account for phenomena normally described by the GM in terms of deformed mean fields. The following is a list of what has been done:

(1) A numerical comparison has been made for FDSM and PRM to further confirm the equivalence of these two models¹⁶⁾. In the calculations one odd particle in an $i_{13/2}$ orbital is considered. On the surface it appears that these two approaches are completely different: the PRM assumes a deformed core with an extra particle moving in the Nilsson potential, while the FDSM starts from the spherical shell model considering n_1 particles interacting by two-body forces in normal-parity levels without introducing any deformation or Nilsson scheme. Nevertheless, the two models essentially arrive at the same results if n_1 is large enough.

(2) It has been shown that the abnormal-parity Nilsson levels in one major shell can be derived from the FDSM in the large n_1 limit¹⁷⁾. For more than one particle in the abnormal level the energy obtained from diagonalizing the FDSM Hamiltonian approaches the sum of Nilsson single-particle energies when n_1 is large enough. Thus we illustrated for the abnormal-parity level how the deformed shell model can be obtained from the spherical shell model via the FDSM. More recently, we have been able to demonstrate a corresponding equivalence for the normal-parity Nilsson levels (unpublished).

(3) Finite particle number effects have been studied¹⁷⁾ (after all, n_1 cannot be infinity for real nuclei). These effects cause a renormalization of the moment of inertia and deformations, and an attenuation of the Coriolis interaction in the PRM.

(4) It has been shown that if the $u \neq 0$ configurations are taken into account the FDSM can describe all the basic features of high-spin phenomena, including rotational alignment, Coriolis antipairing (CAP), band crossings and the associated backbendings¹⁸⁾. For example, the small $B(E2)$ fluctuations at spin 10~20 in the actinide region were first given a plausible explanation by the FDSM.

(5) Finite particle number effects were also demonstrated in high-spin physics. For example, it has been found that finite particle number effects are responsible for the loss of $B(E2)$ strength and the band termination at high spins¹⁹⁾. The FDSM calculation is very simple, but agrees with data very well.

(6) A mean field approximation, the symmetry constrained Hartree-Fock-Bogoliubov method, has been developed for the FDSM²⁰⁾. Using this technique, it is possible to calculate the nuclear energy surface and discuss the nuclear deformed shape within the FDSM context. This method has been applied to rare-earth nuclei. The calculation is much simpler than the traditional HFB, but the results

are comparable and agree with data reasonably well. One consequence is that the dominance of prolate over oblate deformation for rare-earth nuclei can be explained very naturally.

(7) In this paper, for simplicity, pairing has not been considered. This is why the nuclear moment of inertia appears as a constant, $I/2\hbar = a$, as expected for a rigid-rotor. If pairing is taken into account in the FDSM we obtain a result well-known empirically that the moment of inertia is significantly reduced^{2,1)}. This is because the pairing energy in the SU_3 case contains a term $[(G_0 - G_2)] \cdot \frac{(2Q_1/3 - n_1 + 2)}{4(n_1 - 1)} R(R + 1)$, which leads to an effective decrease of the moment of inertia. Furthermore, when the core angular momentum R increases, the Coriolis interaction will lower the $u_1 = 2(3)$ states (the CAP-effect), which leads to an effective increase of moment of inertia through mixing with the ground band; in addition, the pairing term will prefer to have larger n_1 , which physically corresponds to the »stretching effect«, since a larger n_1 will lead to a larger moment of inertia and larger deformation according to Eq. (3.17). Thus the FDSM provides a microscopic understanding of the influence of pairing on the moment of inertia, and of the interplay between pairing, Coriolis, and centrifugal forces in modifying the moment of inertia of yrast band at finite angular momentum.

To conclude, the accumulation of the above mentioned results suggests very strongly that the geometrical model of rotating nuclei is equivalent to a particular limit of the FDSM, the large particle number limit. In this paper, we demonstrate that this equivalence is not restricted to ground band, and first β -band and γ -band, but is true for all β - γ vibrational states. The one-to-one correspondence between β - γ vibrational states and SU_3 representations suggests an inherent relationship between the nuclear collective rotational motion and the SU_3 symmetry of the system in the limit of large particle number. However, if we do not take the large n_1 limit, the FDSM is able to account for finite particle number effects. Since real nuclei are finite many-body systems, we expect that these effects should lead to observable deviation from behaviour expected in the simple geometrical model.

Acknowledgements

We are very grateful for the many useful discussions with B. R. Mottelson, J. P. Draayer, L. L. Riedinger, R. M. Diamond, K. T. Hecht, S. E. Koonin, I. Talmi, S. Levit, F. Sakata, J. Vary, M. Vallieres, W.-M. Zhang, H. Wu and Z.-P. Li. C.-L. Wu would like to express special thanks to Drexel University, the University of Tennessee, and the Joint Institute for Heavy-Ion Research, Oak Ridge National Laboratory, for hosting his profitable stay in the U. S. Research at Drexel University is supported by the U. S. NSF. Research at the University of Tennessee is supported by U. S. DOE under contract no. DE-ASO5-76ER04936. Oak Ridge National Laboratory is operated by Martin Marietta Energy Systems, Inc. for the U. S. DOE under contract no. DE-AC0584OR21400. The Joint Institute for Heavy Ion Research has as member institutions the University of Tennessee, Vanderbilt University, and the Oak Ridge National Laboratory, it is supported by the members and by the DOE through contract no. DE-ASO5-76ERO-4936 with the University of Tennessee. This work is also partially supported by the Chinese Science Foundation.

References

- 1) C.-L. Wu, D. H. Feng, X.-G. Chen, J.-Q. Chen and M. W. Guidry, *Phys. Lett.* **168B** (1986) 313;
- 2) C.-L. Wu, H. D. Feng, X.-G. Chen, J.-Q. Chen and M. W. Guidry, *Phys. Rev.* **C36** (1987) 1157;
- 3) J. N. Ginocchio, *Phys. Rev.* **B29** (1978) 173; *Ann. of Phys.* **176** (1980) 234;
- 4) R. F. Casten, C.-L. Wu, D. H. Feng, J. N. Ginocchio and X.-L. Han, *Phys. Rev. Lett.* **56** (1986) 2578;
- 5) A. Arima and F. Iachello, *Ann. Rev. of Nucl. Part. Sci.* **31** (1981) 75;
- 6) J.-Q. Chen, D. H. Feng and C.-L. Wu, *Phys. Rev.* **C34** (1986) 2269;
- 7) H. Wu and M. Vallieres, *Phys. Rev.* **C39** (1989).
- 8) C.-L. Wu, X. L. Han, Z. P. Li, M. W. Guidry and D. H. Feng, *Phys. Lett.* **B194** (1987) 447; W. M. Zhang, D. F. Feng, C. L. Wu and M. W. Guidry, *J. Phys. G: Nucl. Part. Phys.* **15** (1989) L 115;
- 9) D. H. Feng, C. L. Wu, M. W. Guidry and Z. P. Li, *Phys. Lett.* **B705** (1988) 157;
- 10) See A. Bohr and B. R. Mottelson, *Nuclear Structure*, Vol. I and II (Benjamin), New York, (1975);
- 11) A. Goodman, *Adv. in Nucl. Phys.* Vol. II, ed. J. Negele and E. Vogt, Plenum, NY, 1979;
- 12) K. W. Schmid, Workshop on Microscopic Models in Nuclear Structure Physics (World Scientific), (1988) 315, edited by M. W. Guidry, J. H. Hamilton, D. H. Feng, N. R. Johnson, and J. B. McGrory;
- 13) J. P. Elliott, *Proc. Roy. Soc.* **745A** (1958) 562; D. Vergados, *Nucl. Phys.* **A111** (1968) 681;
- 14) M. Sakai, *Atomic Data and Data Nuclear Tables* **31** (1984) 399–432;
- 15) H. Wu, D. H. Feng, C.-L. Wu and M. W. Guidry, *Phys. Lett.* **198B** (1987) 119;
- 16) H. Wu, D. H. Feng, C.-L. Wu, Z.-P. Li and M. W. Guidry, *Phys. Lett.* **193B** (1987) 169;
- 17) H. Wu, C.-L. Wu, D. H. Feng and M. W. Guidry, *Phys. Rev.* **C32** (1988) 1738;
- 18) M. W. Guidry, C.-L. Wu, D. H. Feng, J. N. Ginocchio, X.-G. Chen and J.-Q. Chen, *Phys. Lett.* **126B** (1986) 1;
- 19) M. W. Guidry, C.-L. Wu, Z.-P. Li, D. H. Feng and J. N. Ginocchio, *Phys. Lett.* **182B** (1986) 210;
- 20) W.-M. Zhang, C.-L. Wu, D. H. Feng, J. N. Ginocchio and M. W. Guidry, *Phys. Rev.* **C38** (1988) 1475;
- 21) J.-Q. Chen, X.-G. Chen, D. H. Feng, C.-L. Wu, J. N. Ginocchio and M. W. Guidry, *Phys. Rev. C* (in press).

β - γ VIBRACIJE I SU(3) SIMETRIJA U MODELU FERMIONSKO
-DINAMIČKE SIMETRIJE

CHENG-LI WU

Department of Physics and Astronomy, Univ. of Tennessee, Knoxville, Tennessee;

Department of Physics and Atmospheric Science, Drexel Univ., Philadelphia, Pennsylvania, USA

MIKE W. GUIDRY

Department of Physics and Astronomy, Univ. of Tennessee, Knoxville, Tennessee, USA

DA HSUAN FENG i JIN QUAN CHEN

Department of Physics and Atmospheric Science, Drexel University, Philadelphia, USA

UDK 539.142

Originalni znanstveni rad

Nadeno je da različita β - γ vibraciona stanja u geometrijskom opisu odgovaraju različitim SU(3) reprezentacijama u FDSM te da postoji veza između β - γ vibracionih kvantnih brojeva (n_3, n_p, K) i SU(3) kvantnih brojeva (λ, μ, K)